Stem Cell Reports
Article

ISSCR

OPEN ACCESS

FGF2 Has Distinct Molecular Functions from GDNF in the Mouse Germline Niche

Kaito Masaki,[1,9] Mizuki Sakai,[2,9] Shunsuke Kuroki,[3] Jun-Ichiro Jo,[4] Kazuo Hoshina,[5] Yuki Fujimori,[5] Kenji Oka,[6] Toshiyasu Amano,[7] Takahiro Yamanaka,[1] Makoto Tachibana,[3] Yasuhiko Tabata,[4] Tanri Shiozawa,[6] Osamu Ishizuka,[8] Shinichi Hochi,[1,2] and Seiji Takashima[1,2,10,*]

[1]Department of Textile Science and Technology, Interdisciplinary Graduate School of Science and Technology, Shinshu University, 3-15-1 Tokida, Ueda 386-8567, Japan
[2]Department of Applied Biology, Faculty of Textile Science and Technology, Shinshu University, Ueda 386-8567, Japan
[3]Division of Epigenome Dynamics, Institute of Advanced Medical Sciences, Tokushima University, Tokushima 770-8501, Japan
[4]Laboratory of Biomaterials, Institute for Frontier Life and Medical Sciences, Kyoto University, Kyoto 606-8507, Japan
[5]Nagano Animal Industry Experiment Station, Shiojiri 399-0711, Japan
[6]Department of Obstetrics and Gynecology, Shinshu University School of Medicine, Matsumoto 390-8621, Japan
[7]Department of Urology, Nagano Red Cross Hospital, Nagano 380-8582, Japan
[8]Department of Urology, Shinshu University School of Medicine, Matsumoto 390-8621, Japan
[9]Co-first author
[10]Senior author
*Correspondence: stakashi@shinshu-u.ac.jp
https://doi.org/10.1016/j.stemcr.2018.03.016

SUMMARY

Both glial cell line-derived neurotrophic factor (GDNF) and fibroblast growth factor 2 (FGF2) are bona fide self-renewal factors for spermatogonial stem cells, whereas retinoic acid (RA) induces spermatogonial differentiation. In this study, we investigated the functional differences between FGF2 and GDNF in the germline niche by providing these factors using a drug delivery system *in vivo*. Although both factors expanded the GFRA1$^+$ subset of undifferentiated spermatogonia, the FGF2-expanded subset expressed RARG, which is indispensable for proper differentiation, 1.9-fold more frequently than the GDNF-expanded subset, demonstrating that FGF2 expands a differentiation-prone subset in the testis. Moreover, FGF2 acted on the germline niche to suppress RA metabolism and GDNF production, suggesting that FGF2 modifies germline niche functions to be more appropriate for spermatogonial differentiation. These results suggest that FGF2 contributes to induction of differentiation rather than maintenance of undifferentiated spermatogonia, indicating reconsideration of the role of FGF2 in the germline niche.

INTRODUCTION

Spermatogonial stem cells (SSCs) are a subpopulation of undifferentiated spermatogonia and the origin of spermatogenesis. They reside in a specialized microenvironment called the germline niche located at the periphery of seminiferous tubules in mammalian testes. The germline niche permits SSCs to produce both stem cells and committed progenitors called differentiating spermatogonia by repeated self-renewal and differentiation. Differentiating spermatogonia further amplify their population by several mitotic divisions and enter meiotic division to produce spermatozoa (de Rooij and Russell, 2000).

It is well established that glial cell line-derived neurotrophic factor (GDNF) ensures the survival and self-renewal of SSCs. Meng et al. (2000) demonstrated that GDNF is indispensable for SSC self-renewal by analyzing *Gdnf* transgenic/deficient mice. Kanatsu-Shinohara et al. (2003) took advantage of GDNF functions to establish cultured SSCs termed germline stem (GS) cells from mouse pup testes. This technique enables identification of cytokines and chemicals that affect the behavior of SSCs.

Our recent study revealed that fibroblast growth factor 2 (FGF2) is another bona fide self-renewal factor for SSCs (Takashima et al., 2015). FGF2-cultured spermatogonia (F-SPG) cultured for more than 4 months under GDNF-free conditions colonized infertile mouse testes and restored fertility by spermatogonial transplantation. Compared with GDNF-cultured spermatogonia (G-SPG), F-SPG exhibit more differentiated characteristics such as lower SSC activity and higher KIT expression in addition to a difference in MAP2K1/2 dependency. These data suggest that FGF2 plays a distinct role in regulating undifferentiated spermatogonia *in vivo*.

It is also known that retinoic acid (RA) is required for spermatogonial differentiation (Hogarth et al., 2011). Of three RA receptor isotypes, retinoic acid receptor γ (RARG) has been reported to specifically contribute to this process (Gely-Pernot et al., 2012). Recently, Ikami et al. (2015) demonstrated that RARG expression is sufficient for induction of RA susceptibility in undifferentiated spermatogonia expressing GFRA1 that triggers GDNF signaling in combination with transmembrane receptor tyrosine kinase RET (Sariola and Saarma, 2003). For further understanding, it should be elucidated how RARG$^+$

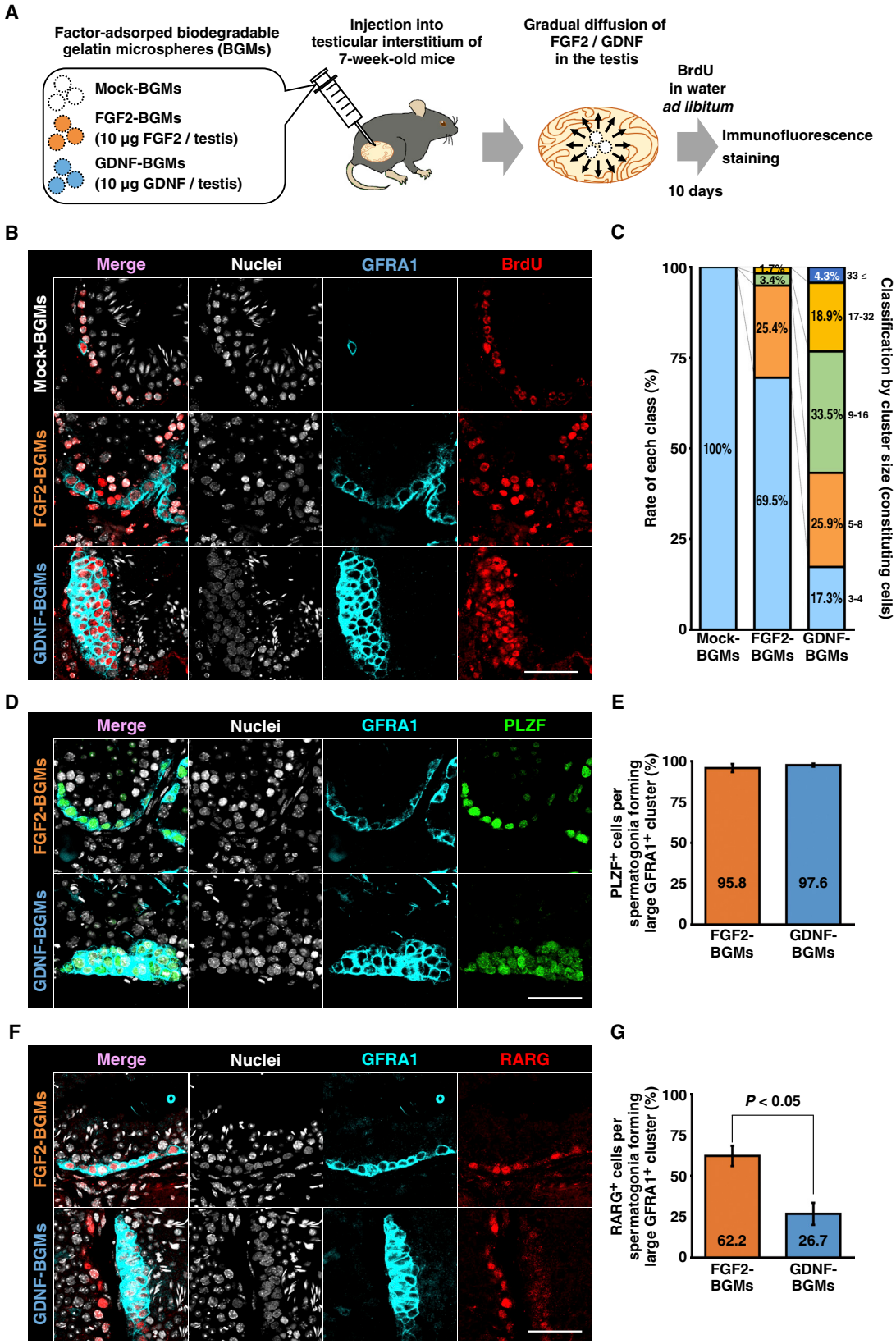

(legend on next page)

spermatogonia are derived from GFRA1$^+$ undifferentiated spermatogonia and how RA signals are regulated within the germline niche.

Although FGF2 is considered to be a possible candidate that induces the RARG$^+$ subset of undifferentiated spermatogonia, the absence of an animal model has hampered the analysis. *Fgf2*-transgenic mice are fertile and not reported to have abnormal testes (Coffin et al., 1995). This is because transgenic mice might not show extremely strong transgene expression depending on the gene. Furthermore, FGF2-knockout mice show no obvious defects in testicular functions (Zhou et al., 1998), which may be because of functional complementation by other FGF molecules.

To overcome such circumstances, we used the biodegradable gelatin microsphere (BGM) system to provide strong FGF2 stimuli only in the testis. This system was established and reported primarily by Tabata et al. (1999). BGMs were prepared by glutaraldehyde-mediated cross-linking of acidic gelatin (microsphere diameter: 30–100 μm). FGF2 can be adsorbed onto BGMs and released depending on the biodegradation of BGMs (Yamamoto et al., 2001). BGMs were first applied to deliver FGF2 into the skin to induce neovascularization (Tabata et al., 1999) and later applied to deliver bone morphogenetic protein 2 and transforming growth factor β1 for heart and bone regeneration (Ueda et al., 2002; Yamamoto et al., 2006; Marui et al., 2007). Uchida et al. (2016) also employed a similar system using different material to induce hyperproliferation of undifferentiated spermatogonia by GDNF treatment, as observed in the previous report of Meng et al. (2000). These reports encouraged employment of the BGM system.

In this study, we analyzed the molecular functions of FGF2 in the mouse germline niche using BGMs for direct FGF2 stimulation *in vivo*. Although we found that FGF2 expanded GFRA1$^+$ spermatogonia, these cells exhibited a phenotype distinct from that of GDNF-expanded GFRA1$^+$ spermatogonia. Moreover, FGF2 modified germline niche functions to be more appropriate for spermatogonial differentiation.

RESULTS

Fgf2 Expression in the Testis

To identify the origin of FGF2 in the testis, we conducted qRT-PCR analyses. For Sertoli cell analysis, we used *R26-CAG-LoxP-hCD271*; *Amh-Cre* mice to purify Sertoli cells by magnetic-activated cell sorting (MACS) (Figure S1A) (Kuroki et al., 2015). Although purified Sertoli cells expressed *Gdnf*, *Fgf2* expression was very low compared with whole testis cells, suggesting that other cell types express *Fgf2* (Figures S1B and S1C). In contrast, germ cell depletion decreased *Fgf2* expression to some extent, suggesting that germ cells and other components of the germline niche express *Fgf2* (Figures S1D and S1E). We also detected FGF2 in the testes of rodents, domestic animals, and humans, suggesting conservation of FGF2 production in mammalian testes (Figure S1F).

FGF2 Expands GFRA1$^+$ Spermatogonia *In Vivo*

We examined the functions of FGF2 in the testis by applying BGMs for continual growth factor stimulation *in vivo* (Figure 1A) (Tabata et al., 1999). Growth factor-adsorbed BGMs were transplanted directly into the testicular interstitium of C57BL6/N mice (7 weeks old) under isoflurane anesthesia. Until sacrifice, bromodeoxyuridine (BrdU) was administered via water *ad libitum* to label proliferating cells. At 10 days after the procedure, BGM-treated testes were harvested and examined by immunofluorescence staining (Figure 1B). Although six testes were included in each group (mock-, FGF2-, and GDNF-BGMs), five testes (mock-BGM), six testes (FGF2-BGM), and four testes (GDNF-BGM) were successfully

Figure 1. FGF2 Expands GFRA1$^+$ Spermatogonia Phenotypically Distinct from Those Induced by GDNF

(A) Flow chart of biodegradable gelatin microsphere (BGM) experiments. Mock-, FGF2-, or GDNF-adsorbed BGMs were bilaterally injected into the interstitium of 7-week-old mouse testes. BrdU was administered via water *ad libitum* until mice were sacrificed. At 10 days after injection, testes were analyzed by immunofluorescence staining. Results were obtained independently from three mice.

(B and C) Cluster formation and proliferation of GFRA1$^+$ spermatogonia induced by BGM transplantation. (B) Immunofluorescence staining. GFRA1 and incorporated BrdU are visualized by cyan and red, respectively. Nuclei were counterstained with Hoechst 33,342 (gray). (C) Classification of large GFRA1$^+$ clusters by the number of constituting spermatogonia. Mock-BGMs, n = 5 testes; FGF2-BGMs, n = 6 testes; GDNF-BGMs, n = 4 testes. A total of 1,434 tubules with 261 large GFRA1$^+$ clusters carrying 2749 GFRA1$^+$ spermatogonia were analyzed.

(D–G) Characterization of BGM-induced large GFRA1$^+$ clusters. (D and E) PLZF expression in large GFRA1$^+$ clusters. (D) Immunofluorescence staining. GFRA1 is visualized by cyan, while PLZF is visualized by green. Nuclei were counterstained with Hoechst 33,342 (gray). (E) Quantitative analysis of PLZF expression in large GFRA1$^+$ clusters. FGF2-BGMs, n = 5 testes; GDNF-BGMs, n = 4 testes. A total of 957 tubules with 190 large GFRA1$^+$ clusters carrying 2,111 GFRA1$^+$ spermatogonia were analyzed. In this experiment, one FGF2-BGM-treated testis, which did not carry large GFRA1$^+$ clusters, was excluded from the statistical analysis. (F and G) RARG expression in large GFRA1$^+$ clusters. (F) Immunofluorescence staining. GFRA1 is visualized by cyan, while RARG is visualized by red. Nuclei were counterstained with Hoechst 33,342 (gray). (G) Quantitative analysis of RARG expression in large GFRA1$^+$ clusters. FGF2-BGMs, n = 6 testes; GDNF-BGMs, n = 4 testes. A total of 1,347 tubules with 214 large GFRA1$^+$ clusters carrying 2,147 GFRA1$^+$ spermatogonia were analyzed.

Results are presented as means ± SEM. Scale bars, 50 μm (B, D, and F). See also Figures S1 and S2; Table S1.

transplanted with BGMs. Testes were harvested independently from three mice for each group.

In adult mice, most GFRA1$^+$ spermatogonia exist as single or paired cells, and spermatogonial clusters consisting of three or more cells are rare (Suzuki et al., 2009; Nakagawa et al., 2010; Grasso et al., 2012). In agreement with these previous studies, transplantation of mock-BGMs had no effect on GFRA1$^+$ spermatogonia. Most GFRA1$^+$ spermatogonia were found as single or paired cells (Figure 1B). Next, we defined GFRA1$^+$ spermatogonial clusters consisting of three or more cells as "large GFRA1$^+$ clusters." In this regard, we also classified large GFRA1$^+$ clusters into five classes based on the number of constituting GFRA1$^+$ spermatogonia (Figures 1C and S2A). We found only 17 large GFRA1$^+$ clusters consisting of three or four spermatogonia in 507 tubule sections from five testes (Figure 1C).

GDNF-BGMs often induced large GFRA1$^+$ clusters exhibiting a multi-layered, dome-like morphology (Figures 1B, S2A, and S2B). This result is consistent with a previous report showing that intratesticular transplantation of GDNF-soaked beads induces hyperproliferation of GFRA1$^+$ spermatogonia (Uchida et al., 2016). A total of 185 large GFRA1$^+$ clusters were found in 457 tubule sections from four testes, and 82.7% (153/185) of clusters consisted of more than four spermatogonia (Figure 1C). Although FGF2-BGMs also induced large GFRA1$^+$ clusters, these cells were prone to form two-dimensional flat colonies along the basement membrane of seminiferous tubules (Figures 1B and S2A–S2D). Fifty-nine large GFRA1$^+$ clusters were found in 470 tubule sections from six testes, and 30.5% (18/59) of them consisted of more than four spermatogonia (Figure 1C). In the most extreme case, GFRA1$^+$ spermatogonia covered the entire circumference of the seminiferous tubule (Figure S2D). In GDNF- and FGF2-BGM-treated testes, large GFRA1$^+$ clusters were prone to reside adjacent to BGMs (Figures S2B–S2D). We also observed that GFRA1$^+$ spermatogonia that formed large clusters frequently incorporated BrdU (Figure 1B). These data strongly suggest that FGF2 also acts as growth factor for GFRA1$^+$ spermatogonia.

Phenotypic Differences between FGF2- and GDNF-Expanded GFRA1$^+$ Spermatogonia

We also found morphological differences between FGF2- and GDNF-expanded large GFRA1$^+$ clusters, suggesting functional differences of these factors. Therefore, we compared the phenotypes of FGF2- and GDNF-expanded GFRA1$^+$ spermatogonia that formed large clusters. We found some large GFRA1$^+$ clusters in mock-BGM-treated testes. However, consistent with previous reports (Suzuki et al., 2009; Nakagawa et al., 2010), the number of large GFRA1$^+$ clusters was inadequate for statistical analysis. Therefore, mock-BGM samples were omitted, and comparisons of FGF2-BGM and GDNF-BGM samples were conducted. In this experiment, we examined expression of two spermatogonial markers, promyelocytic leukemia zinc finger (PLZF) protein (marker for undifferentiated spermatogonia) and RARG (marker for a subset of undifferentiated spermatogonia and differentiating spermatogonia). The former is expressed in a broad range of undifferentiated spermatogonia and is essential for their maintenance (Buaas et al., 2004; Costoya et al., 2004). The latter can monitor the differentiation of GFRA1$^+$ undifferentiated spermatogonia into differentiating spermatogonia and is necessary and sufficient for acquisition of RA signals for differentiation into differentiating spermatogonia (Gely-Pernot et al., 2012; Ikami et al., 2015). Ikami et al. (2015) demonstrated that genetically modified GFRA1$^+$ spermatogonia expressing RARG are persistently competent for RA-mediated spermatogonial differentiation. Therefore, RARG/*Rarg* is considered to be an appropriate marker to monitor the differentiation of GFRA1$^+$ spermatogonia. Immunofluorescence staining revealed that both populations exhibited the PLZF$^+$ phenotype typical for undifferentiated spermatogonia (Figures 1D and 1E). However, a greater percentage of FGF2-expanded GFRA1$^+$ spermatogonia expressed RARG than cells expanded with GDNF (Figures 1F and 1G). In this regard, Ikami et al. (2015) also identified the "GFRA1$^+$RARG$^+$ subset" of undifferentiated spermatogonia as an intermediate between the GFRA1$^+$ primitive subset and more differentiated *Neurog3*-EGFP$^+$ (RARG/*Rarg*) subset. Considering that RARG is indispensable for proper spermatogonial differentiation (Gely-Pernot et al., 2012), FGF2 might expand a differentiating subset of GFRA1$^+$ spermatogonia.

FGF2 Is Functionally More Permissive for *Rarg* Expression

Next, we examined how the GFRA1$^+$RARG$^+$ subset was expanded. Undifferentiated spermatogonia can be divided into GFRA1$^+$ and GFRA1$^-$ subsets (Garbuzov et al., 2018). The GFRA1$^+$ subset possesses a higher SSC frequency and a more immature phenotype than the GFRA1$^-$ subset, and the GFRA1$^-$ subset can produce the GFRA1$^+$ subset (Figure 2A). Hara et al. (2014) also observed a similar phenomenon whereby the GFRA1$^+$ subset produces a *Neurog3*-EGFP$^+$ subset and the latter can produce the former. Based on these contexts, we hypothesized three possible mechanisms that expand the GFRA1$^+$ RARG$^+$ subset: (1) FGF2 induces RARG expression in the GFRA1$^+$RARG$^-$ subset; (2) FGF2 expands the GFRA1$^+$ RARG$^+$ subset within the GFRA1$^+$ undifferentiated spermatogonial population; and (3) FGF2 induces reversion of GFRA1-undifferentiated spermatogonia into the GFRA1$^+$RARG$^+$ subset. To test the former two hypotheses, we employed SSC cell lines, GS cells, F-SPG, and G-SPG.

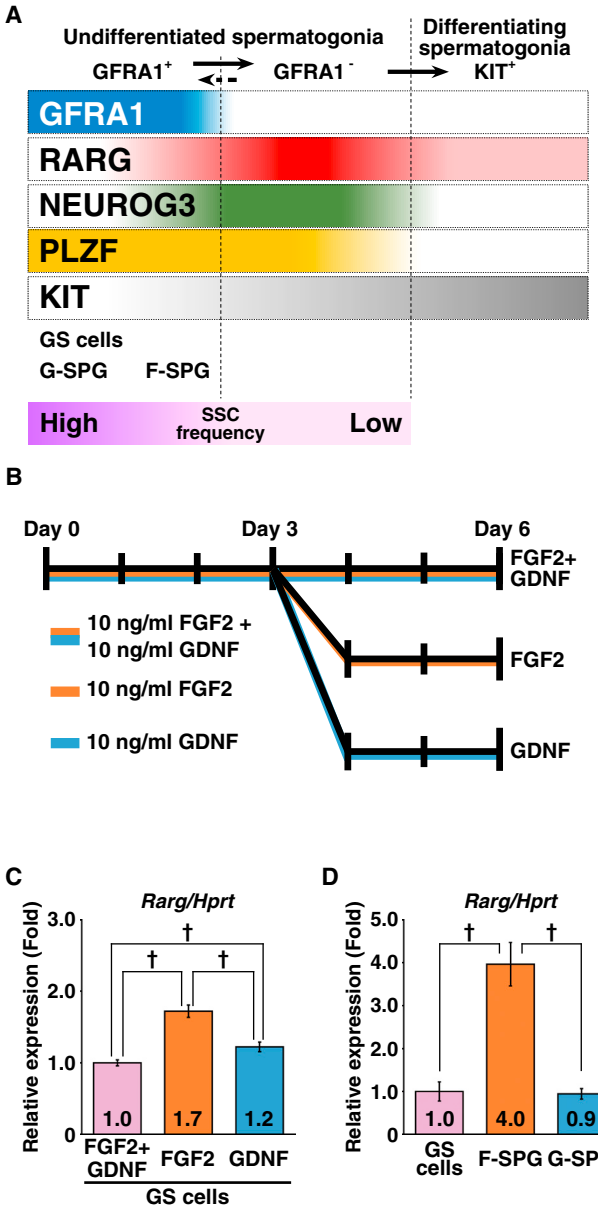

Figure 2. FGF2 Is Permissive for *Rarg* Expression in Cultured Spermatogonial Cell Lines

(A) Schematic representation of the phenotype of spermatogonial subsets and SSC cell lines based on previous reports (Gely-Pernot et al., 2012; Hara et al., 2014; Ikami et al., 2015; Takashima et al., 2015; Garbuzov et al., 2018).

(B and C) Effects of FGF2 and GDNF on *Rarg* expression in GS cells. (B) GS cell culture conditions. Cells were cultured on laminin-coated dishes. (C) qRT-PCR analysis. After normalization to *Hprt* expression, values of FGF2 + GDNF were set to 1.0 (n = 8 independent cultures for each group).

(D) qRT-PCR analysis of *Rarg* expression in cultured spermatogonial cell lines. After normalization to *Hprt* expression, the value of GS cells was set to 1.0 (GS cells, n = 13 independent cultures; F-SPG, n = 14 independent cultures; G-SPG, n = 18 independent cultures).

These cells are powerful tools for biochemical and molecular analyses of undifferentiated spermatogonia (Kanatsu-Shinohara et al., 2003; Takashima et al., 2015). GS cells were established and maintained consistently with both GDNF and FGF2, while F-SPG and G-SPG were established and maintained consistently with FGF2 or GDNF, respectively. Considering the persistent expression of GFRA1 in culture, these cells recapitulated the characteristics of the GFRA$^+$ subset of undifferentiated spermatogonia (Figure 2A).

First, we cultured GS cells on laminin-coated dishes with or without the two growth factors and found that growth factor stimulation suppressed *Rarg* in GS cells (Figures S3A and S3B). Next, we determined which factor suppressed *Rarg* in GS cells. After deprivation of growth factors for 2 days, GS cells were cultured for another 2 days with FGF2 and/or GDNF at various concentrations. This experiment revealed that both factors had a *Rarg*-suppressive activity, and the concentration or combination of the two factors did not show any change in suppression of *Rarg* (Figures S3C and S3D). However, GS cells cultured under GDNF-free conditions for 3 days (orange column) expressed higher levels of *Rarg* than those cultured under FGF2-free (blue column) or FGF2 + GDNF (purple column) conditions (Figures 2B and 2C). Considering that F-SPG expressed a higher level of *Rarg* than GS cells and G-SPG (Figure 2D), it is likely that FGF2 is more permissive than GDNF for expression of *Rarg*/RARG in GFRA1$^+$ spermatogonia.

FGF2 Acts on the Germline Niche to Suppress GDNF and Permits RA Actions

We also determined FGF2 functions in the germline niche. In this experiment, we used the testes of busulfan-treated mice, because *Fgf2* expression is attenuated and the germline niche remains functional. However, we did not examine GDNF functions because GFRA1 is expressed exclusively in undifferentiated spermatogonia of mouse testes (Figures S2A–S2D). Mock- or FGF2-BGMs were transplanted into testes of busulfan-treated mice, and the testes were harvested at 1 or 10 days after transplantation. Gene expression related to germline niche functions was assessed by qRT-PCR and western blotting (Figure 3A).

Although we analyzed BGM-transplanted testes harvested at 10 days after the procedure, almost all injected FGF2 had disappeared (Figure S4A). This result was different from a study indicating that BGMs continue to release FGF2 *in vivo* for up to 14 days after the procedure (Yamamoto et al., 2001). In this situation, gene expression

Results were obtained from three (GS cells and F-SPG) and four (G-SPG) independently established sublines for each group.

Results are presented as means ± SEM. Daggers indicate statistical significance ($^{\dagger}p < 0.05$).

See also Figure S3 and Table S2.

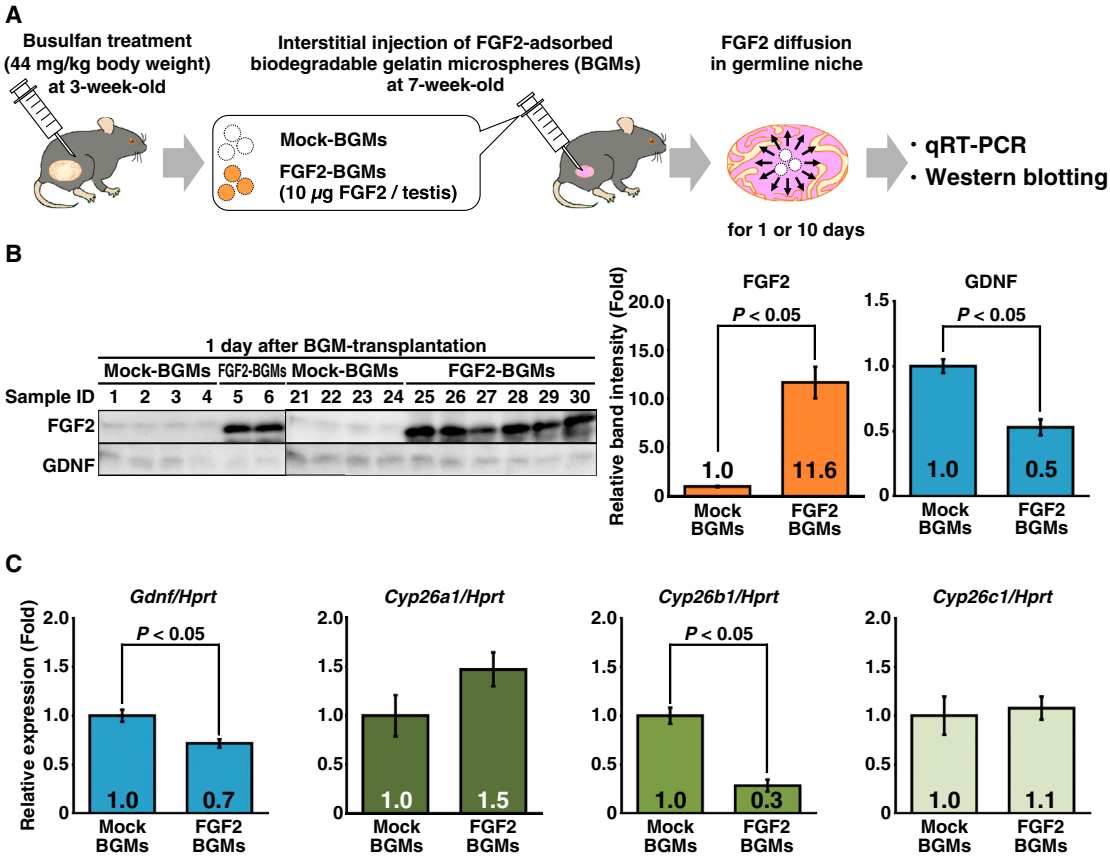

Figure 3. FGF2 Acts on the Germline Niche to Suppress *Gdnf*/GDNF and *Cyp26b1*

(A) Flow chart of the BGM experiment to assess FGF2 functions in the germline niche. Busulfan-treated testes, in which germ cells are depleted and germline niches remain functional, were used in this analysis. At 1 or 10 days after BGM transplantation, testes were harvested and analyzed by qRT-PCR and western blotting.

(B) Western blot analyses of testes at 1 day after BGM treatment. Band intensities of the Mock-BGM group were set to 1.0 (n = 8 testes for each condition).

(C) qRT-PCR analysis of testes at 1 day after BGM treatment. After normalization to *Hprt* expression, values of the Mock-BGM group were set to 1.0 (n = 8 testes for each condition).

Results are presented as means ± SEM. See also Figure S4; Tables S1 and S2.

related to germline niche functions was unchanged (Figure S4B). However, this BGM system was supposed to be adequate to assess the molecular functions of FGF2 in the germline niche, because this procedure succeeded in inducing hyperproliferation of GFRA1$^+$ spermatogonia by GDNF/FGF2 (Figures 1B, 1C, and S2A–S2D). In contrast, testes harvested at 1 day after the procedure still retained a substantial and non-physiological amount of FGF2, and *Gdnf*/GDNF was downregulated (Figures 3B and 3C). These results are consistent with our previous report showing that *Fgf2* knockdown in mouse testes induces GDNF production (Takashima et al., 2015). Moreover, we found suppression of *Cyp26b1* that encodes an RA-metabolizing enzyme (Figure 3C). Although the role of *Cyp26c1* in mice remains to be elucidated, considering that deficiency of *Cyp26b1*, but not *Cyp26a1*, in Sertoli cells compromises spermatogenesis (Hogarth et al., 2015a), it has been suggested that FGF2 plays an important role in regulating RA metabolism in the germline niche by regulating *Cyp26b1*. To further understand the regulation of *Gdnf* and *Cyp26* genes, we assessed RA functions in the germline niche. In this experiment, busulfan-treated mice were intraperitoneally injected with 750 μg of RA and their testes were harvested at 11 hr after treatment. qRT-PCR analysis revealed that *Cyp26a1* and *Cyp26c1* were induced by RA while *Cyp26b1* was unaffected, suggesting that *Cyp26b1* is specifically regulated by FGF2 in the germline niche (Figure S4C). RA injection also suppressed *Gdnf*, which is consistent with a previous study (Hasegawa et al., 2013). Taken together, these results suggest that FGF2 modifies germline niche

functions to be more appropriate for spermatogonial differentiation by suppressing GDNF and RA metabolism.

DISCUSSION

We investigated the functions of FGF2 in the germline niche. Although FGF2 expanded GFRA1$^+$ spermatogonia *in vivo*, these cells exhibited a more differentiated phenotype (RARG expression) than those expanded by GDNF. Moreover, FGF2 suppressed RA metabolism and GDNF production. These results suggest that FGF2 acts on both GFRA1$^+$ spermatogonia and their niche to facilitate spermatogonial differentiation, despite the fact that FGF2 is a bona fide self-renewal factor for SSCs.

We applied BGMs for sustained stimulation by growth factors *in vivo*. Although our previous report employed lentivirus-mediated *Fgf2* overexpression in testes (Takashima et al., 2015), it was difficult to judge whether it was sufficient for functional analysis. In contrast, Uchida et al. (2016) demonstrated that transplantation of GDNF-soaked beads induces expansion of GFRA1$^+$ spermatogonia. This observation led us to apply this procedure using BGMs.

BGM performance *in vivo* has already been demonstrated in several studies. In mouse dermal tissue, BGMs achieved prolonged FGF2 release for 14 days and induced angiogenesis, while 80% of FGF2 disappeared from the site of injection within 24 hr, and angiogenesis was not induced without using BGMs (Yamamoto et al., 2001). Based on these observations, we applied this system to achieve prolonged FGF2 stimuli in the testis. Although our data demonstrated that most of the injected FGF2 was consumed by 10 days after the procedure, a substantial amount of FGF2 remained at 1 day after the procedure. Even though this system might not perform as intended (expected stimuli for about 2 weeks), FGF2 stimulation induced hyperproliferation of GFRA1$^+$ undifferentiated spermatogonia and modulated gene expression in the germline niche. Considering that release kinetics are different depending on the growth factor (Yamamoto et al., 2001), it is anticipated that the release kinetics of GDNF are also different from those of FGF2. Hence, it is not appropriate to determine which factor is superior to induce spermatogonial growth using the BGM system.

Using BGMs, although we found that FGF2 expanded GFRA1$^+$ spermatogonia, their number and size were less than those of GDNF-expanded GFRA1$^+$ spermatogonia. This result might be biased by two technical reasons. One might be undefined release kinetics of factors from BGMs as described above. Another is the choice of analytical method for large GFRA1$^+$ clusters. Although we applied whole-mount immunofluorescence to analyze testicular tubules, synechia between seminiferous tubules and BGMs hampered analysis of colonies formed beneath BGMs. Simple observation of frozen sections could not render the whole architecture of colonies. The axis of a tubule section might affect the result of the size and number of large GFRA1$^+$ clusters. However, we succeeded in obtaining colony images without collapsing their structure. Therefore, our data regarding the number and size of large GFRA1$^+$ clusters might be underestimated. Based on these circumstances, our study was limited to comparison of the characteristics of resultant colonies induced by FGF2 or GDNF.

Both FGF2 and GDNF induced morphologically distinct large GFRA1$^+$ clusters *in vivo*. GDNF-BGMs induced multilayered clusters that were morphologically similar to G-SPG, whereas FGF2-BGMs induced flat colonies on the basement membrane of seminiferous tubules, which were similar to F-SPG (Takashima et al., 2015). Our recent report revealed that F-SPG have a more differentiated phenotype without losing their SSC properties. These findings suggest that FGF2-expanded GFRA1$^+$RARG$^+$ spermatogonia *in vivo* might have a more differentiated phenotype. Indeed, Ikami et al. (2015) demonstrated the existence of GFRA$^+$ RARG$^+$ spermatogonia, and that these cells are more susceptible than GFRA1$^+$RARG$^-$ spermatogonia to RA-induced differentiation toward KIT$^+$ differentiating spermatogonia. These observations support our speculation that FGF2 might facilitate spermatogonial differentiation by expanding differentiation-prone GFRA1$^+$RARG$^+$ spermatogonia (Figures 4A and 4B).

An important remaining issue is how FGF2 expands the GFRA1$^+$RARG$^+$ subset of undifferentiated spermatogonia. We determined whether FGF2 induced *Rarg* expression in GFRA1$^+$ spermatogonia using cultured spermatogonial cell lines. In contrast to our expectation, although FGF2 suppressed *Rarg* in GS cells, FGF2 was relatively more permissive for *Rarg* expression than GDNF. These data strongly suggest that FGF2 does not induce *Rarg* in GFRA1$^+$ spermatogonia *in vivo*, rejecting the hypothesis that FGF2 induces *Rarg* expression in GFRA1$^+$ spermatogonia. Considering that FGF2 induces proliferation of undifferentiated spermatogonia, it is considered that at least some GFRA1$^+$RARG$^+$ spermatogonia are expanded by the proliferation of GFRA1$^+$RARG$^+$ spermatogonia themselves. Validation of the third hypothesis, that the GFRA1$^+$RARG$^+$ subset is derived from the GFRA1$^-$ subset via FGF2 stimuli, still remains to be clarified. Although how FGF2 suppresses GDNF in the germline niche (directly or through the CYP26B1-RA pathway) remains unknown, FGF2-mediated GDNF suppression might also contribute to expanding the GFRA1$^+$RARG$^+$ subset.

Which cells produce FGF2 in the testis has been controversial. Some reports demonstrated that Sertoli cells

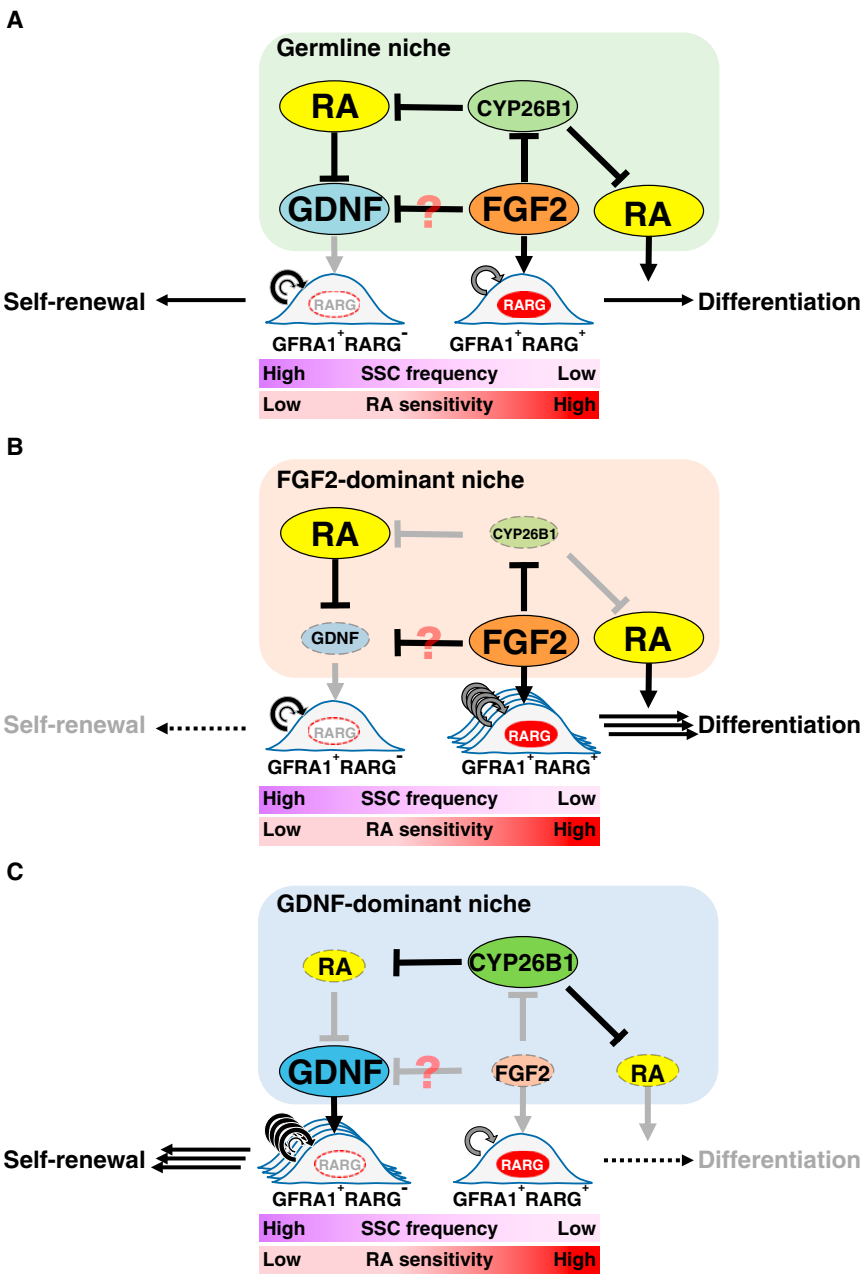

Figure 4. Putative Role of FGF2 in the Mouse Germline Niche

(A) Molecular functions of FGF2 in the germline niche. GDNF expands GFRA1$^+$ RARG$^-$ spermatogonia, whereas FGF2 expands GFRA1$^+$RARG$^+$ spermatogonia that are a differentiation-prone subset (Ikami et al., 2015). Simultaneously, FGF2 also acts on the germline niche to facilitate RA actions via *Cyp26b1* suppression. GDNF suppression might also contribute to expanding GFRA1$^+$RARG$^+$ spermatogonia.

(B and C) The FGF2-dominant niche is prone to differentiation because of permissiveness for expansion of GFRA1$^+$RARG$^+$ spermatogonia and RA actions (B), whereas the GDNF-dominant niche is prone to regeneration (C). Indeed, transplanted undifferentiated spermatogonia are prone to proliferation rather than differentiation in germ cell-depleted testes (Nagano et al., 1999; Nagai et al., 2012; Zohni et al., 2012). The present study also demonstrated that busulfan-mediated germ cell depletion increased the *Gdnf/Fgf2* ratio in the testis (Figure S1).

See also Figure S1.

produce FGF2 (Smith et al., 1989; Mullaney and Skinner, 1992; Tadokoro et al., 2002), whereas others showed that germ cells produce FGF2 (Han et al., 1993; Zhang et al., 2012). Our results demonstrated that Sertoli cells are not the main origin of FGF2, at least under physiological conditions. Subsequent experiments revealed that germ cell depletion attenuated *Fgf2* expression in the testis. Considering that germ cell-free *Nanos3*-knockout mice also show decreased *Fgf8* expression in the testis (Hasegawa and Saga, 2014), *Fgf8* and *Fgf2* might be expressed in a similar manner. There are three possible explanations for this outcome. (1) Germ cells express *Fgf2*, and germ cell depletion causes loss of *Fgf2*. (2) The germline niche expresses *Fgf2* depending on the germ cell-derived signal (JAG1-NOTCH2 pathway) (Garcia et al., 2014), and germ cell depletion attenuates *Fgf2* expressed in the germline niche. (3) Busulfan treatment suppresses *Fgf2* in the germline niche. Direct analysis of purified testis component cells is more likely to identify the *Fgf2*-expressing cells. However, busulfan-mediated expression changes of *Fgf2* and *Gdnf* might be important in understanding the niche function. Germ cell depletion changes the *Gdnf/Fgf2* balance to

modify the functions of the germline niche from a physiological niche to a *Gdnf*-dominant niche appropriate for regeneration (Figures 4A–4C).

We also found that FGF2, but not RA, regulated *Cyp26b1* in the germline niche. Hogarth et al. (2015a) demonstrated that Sertoli cell-expressed *Cyp26b1* is indispensable for proper spermatogenesis, whereas *Cyp26a1* deficiency in Sertoli cells does not cause any spermatogenic defects. Although it remains unclear whether *Cyp26c1* deficiency affects fertility (Uehara et al., 2007), *Cyp26b1* regulated by FGF2 might play an important role in regulating RA actions in the germline niche (Figures 4A and 4B). In this regard, Garcia et al. (2014) reported that germ cell-derived NOTCH signaling is required for proper spermatogenesis, which regulates *Cyp26b1* and *Gdnf* in Sertoli cells. They proposed a model in which the population size of germ cells expressing NOTCH ligands affects the functions of Sertoli cells expressing *Gdnf* and *Cyp26b1*. It is intriguing how germ cells themselves regulate their differentiation dynamics via FGF2 and NOTCH pathways. Additionally, it is well known that RA is the master regulator of the seminiferous epithelial cycle (Hogarth et al., 2013). The RA concentration in testes is determined by the balance between RA production and metabolism (Hogarth et al., 2011). Furthermore, the length of the seminiferous epithelial cycle varies depending on the animal species and is determined by the germ cell genotype (França et al., 1998; Sugimoto et al., 2012). Therefore, it is also intriguing to speculate that germ cell-derived FGF2/NOTCH signals might define the length of the seminiferous epithelial cycle by regulating RA actions in the germline niche.

Our results can explain the functional differences between FGF2 and GDNF. In fact, FGF2 possesses a molecular function that permits RA-mediated differentiation by inducing differentiation-prone GFRA1^{+}RARG^{+} spermatogonia. FGF2 also acts on the germline niche to facilitate RA actions for spermatogonial differentiation (Figure 4A). Previous reports suggest cyclical fluctuation of GDNF and RA in testicular tubules throughout the seminiferous epithelial cycle under physiological conditions (Grasso et al., 2012; Hogarth et al., 2015b). Furthermore, germ cell-deficient conditions are reported to be appropriate for proliferation of undifferentiated spermatogonia rather than spermatogonial differentiation (Nagano et al., 1999; Nagai et al., 2012). Indeed, busulfan treatment upregulates *Gdnf* expression in the testis (Figure S1) (Zohni et al., 2012). These findings suggest the existence of GDNF- and FGF2-dominant niches. The former is considered to promote the proliferation of undifferentiated spermatogonia including SSCs (Figure 4C). Previous reports have demonstrated that transplanted SSCs appear to focus on expansion of their population without production of differentiating progeny in the germ cell-depleted recipient testis (Nagano et al., 1999; Nagai et al., 2012). Our present study also showed a change in the *Gdnf/Fgf2* balance in the germline niche after germ cell depletion by busulfan (Figures S1D and S1E). Considering the phenotype of *Gdnf*-transgenic mice and GDNF-BGM-treated testes, a GDNF-dominant niche might not permit spermatogonial differentiation. In contrast, an FGF2-dominant niche is considered to permit production of GFRA1^{+}RARG^{+} spermatogonia for spermatogenesis (Figure 4B). However, FGF2 signals are not sufficient, and GDNF signals are indispensable for SSC maintenance (Meng et al., 2000). Although FGF2 expression dynamics remain to be elucidated in seminiferous tubules, it is intriguing to speculate that the physiological germline niche shifts cyclically between FGF2- and GDNF-dominant states. For a complete overview of spermatogonial dynamics in the germline niche, it is indispensable to understand spatiotemporal regulation of FGF2 as well as GDNF and RA.

EXPERIMENTAL PROCEDURES

The institutional animal care and use committee of Shinshu University (approval nos. 260013 and 280120) and Tokushima University (experimental number 14,108) approved all animal experimentation protocols. Human testis tissues without pathological lesions were obtained and subjected to the experiments in accordance with the institutional ethics review board of Shinshu University to use human-derived material (test no. 3039), and the institutional ethics review board of Nagano Red Cross Hospital to use human-derived material (Nagano-Byo-Ki approval no. 25). Written consent was obtained following the committee-approved protocol before tissue collection.

Growth Factor Adsorption of BGMs

BGMs were prepared according to the original report (Tabata et al., 1999). For single testis treatment, freeze-dried BGMs (1 mg) were reconstituted with 10 μL of 1 mg/mL recombinant murine FGF2 or GDNF (PeproTech, London, UK) in distilled-deionized-autoclaved water. In this manner, growth factor solutions were completely absorbed in BGMs, demonstrating that the growth factors were entirely contained within BGMs. After overnight adsorption of growth factors at 4°C, the resultant BGMs were suspended in 15 μL of autoclaved physiological saline for transplantation.

Statistical Analyses

Results are presented as means ± SEM. Significance of differences between means for single comparisons was determined by the Student's t test. Multiple comparison analyses were carried out using one-way ANOVA followed by Tukey's honest significant difference test. $p < 0.05$ was considered statistically significant.

SUPPLEMENTAL INFORMATION

Supplemental Information includes Supplemental Experimental Procedures, four figures, and two tables and can be found with this article online at https://doi.org/10.1016/j.stemcr.2018.03.016.

AUTHOR CONTRIBUTIONS

S.T. conceived the concept, designed and performed the experiments, analyzed the data, wrote the manuscript, and secured funding. K.M. performed experiments, analyzed the data, and secured funding. M.S. performed experiments and analyzed the data. S.K. performed experiments. J.-I.J., K.H., Y.F., K.O., T.A., T.Y., M.T., Y.T., T.S., O.I., and S.H. provided reagents.

ACKNOWLEDGMENTS

We thank T. Shinohara (Kyoto University) for generously providing GS cells, F-SPG, and G-SPG, KEYENCE (Osaka, Japan) for use of the BZ-X700 fluorescence microscope, H. Ogawa, Y. Kawahara, H. Adachi, M. Tone, S. Aiba, A. Tsuchimoto, T. Abe, D. Takemasa, A. Miura, and A. Nakano of S.T.'s laboratory for technical assistance and helpful discussions, and Mitchell Arico from Edanz Group (www.edanzediting.com/ac) for editing a draft of this manuscript. This work was funded by JSPS KAKENHI (JP16H05046), The Sumitomo Foundations (no.140785), The Naito Foundation (no. 4342-110), The Ito Foundation (no. Ken 16), The Hokuto Foundation for Bioscience, the Japan Health Foundation (no. 2016-3-145), the Mochida Memorial Foundation for Medical and Pharmaceutical Research, The Ichiro Kanehara Foundation for the Promotion of Medical Sciences and Medical Care, The Uehara Memorial Foundation, the Suzuken Memorial Foundation, the Takeda Science Foundation (to S.T.), and The Foundation of Nagano Prefecture Science Promotion (to K.M.).

Received: April 23, 2017
Revised: March 19, 2018
Accepted: March 20, 2018
Published: April 19, 2018

REFERENCES

Buaas, F.W., Kirsh, A.L., Sharma, M., McLean, D.J., Morris, J.L., Griswold, M.D., de Rooij, D.G., and Braun, R.E. (2004). Plzf is required in adult male germ cells for stem cell self-renewal. Nat. Genet. *36*, 647–652.

Coffin, J.D., Florkiewicz, R.Z., Neumann, J., Mort-Hopkins, T., Dorn, G.W., Lightfoot, P., German, R., Howles, P.N., Kier, A., O'Toole, B.A., et al. (1995). Abnormal bone growth and selective translational regulation in basic fibroblast growth factor (FGF-2) transgenic mice. Mol. Biol. Cell *6*, 1861–1873.

Costoya, J.A., Hobbs, R.M., Barna, M., Cattoretti, G., Manova, K., Sukhwani, M., Orwig, K.E., Wolgemuth, D.J., and Pandolfi, P.P. (2004). Essential role of Plzf in maintenance of spermatogonial stem cells. Nat. Genet. *36*, 653–659.

de Rooij, D.G., and Russell, L.D. (2000). All you wanted to know about spermatogonia but were afraid to ask. J. Androl. *21*, 776–798.

França, L.R., Ogawa, T., Avarbock, M.R., Brinster, R.L., and Russell, L.D. (1998). Germ cell genotype controls cell cycle during spermatogenesis in the rat. Biol. Reprod. *59*, 1371–1377.

Garbuzov, A., Pech, M.F., Hasegawa, K., Sukhwani, M., Zhang, R.J., Orwig, K.E., and Artandi, S.E. (2018). Purification of GFRα1$^+$ and GFRα1$^-$ spermatogonial stem cells reveals a niche-dependent mechanism for fate determination. Stem Cell Reports *10*, 553–567.

Garcia, T.X., Farmaha, J.K., Kow, S., and Hofmann, M.C. (2014). RBPJ in mouse Sertoli cells is required for proper regulation of the testis stem cell niche. Development *141*, 4468–4478.

Gely-Pernot, A., Raverdeau, M., Célébi, C., Dennefeld, C., Feret, B., Klopfenstein, M., Yoshida, S., Ghyselinck, N.B., and Mark, M. (2012). Spermatogonia differentiation requires retinoic acid receptor γ. Endocrinology *153*, 438–449.

Grasso, M., Fuso, A., Dovere, L., de Rooij, D.G., Stefanini, M., Boitani, C., and Vicini, E. (2012). Distribution of GFRA1-expressing spermatogonia in adult mouse testis. Reproduction *143*, 325–332.

Han, I.S., Sylvester, S.R., Kim, K.H., Schelling, M.E., Venkateswaran, S., Blanckaert, V.D., McGuinness, M.P., and Griswold, M.D. (1993). Basic fibroblast growth factor is a testicular germ cell product which may regulate Sertoli cell function. Mol. Endocrinol. *7*, 889–897.

Hara, K., Nakagawa, T., Enomoto, H., Suzuki, M., Yamamoto, M., Simons, B.D., and Yoshida, S. (2014). Mouse spermatogenic stem cells continually interconvert between equipotent singly isolated and syncytial states. Cell Stem Cell *14*, 658–672.

Hasegawa, K., Namekawa, S.H., and Saga, Y. (2013). MEK/ERK signaling directly and indirectly contributes to the cyclical self-renewal of spermatogonial stem cells. Stem Cells *31*, 2517–2527.

Hasegawa, K., and Saga, Y. (2014). FGF8-FGFR1 signaling acts as a niche factor for maintaining undifferentiated spermatogonia in the mouse. Biol. Reprod. *91*, 145.

Hogarth, C.A., Amory, J.K., and Griswold, M.D. (2011). Inhibiting vitamin A metabolism as an approach to male contraception. Trends Endocrinol. Metab. *22*, 136–144.

Hogarth, C.A., Evanoff, R., Mitchell, D., Kent, T., Small, C., Amory, J.K., and Griswold, M.D. (2013). Turning a spermatogenic wave into a tsunami: synchronizing murine spermatogenesis using WIN 18,446. Biol. Reprod. *88*, 40.

Hogarth, C.A., Evans, E., Onken, J., Kent, T., Mitchell, D., Petkovich, M., and Griswold, M.D. (2015a). CYP26 enzymes are necessary within the postnatal seminiferous epithelium for normal murine spermatogenesis. Biol. Reprod. *93*, 19.

Hogarth, C.A., Arnold, S., Kent, T., Mitchell, D., Isoherranen, N., and Griswold, M.D. (2015b). Processive pulses of retinoic acid propel asynchronous and continuous murine sperm production. Biol. Reprod. *92*, 37.

Ikami, K., Tokue, M., Sugimoto, R., Noda, C., Kobayashi, S., Hara, K., and Yoshida, S. (2015). Hierarchical differentiation competence in response to retinoic acid ensures stem cell maintenance during mouse spermatogenesis. Development *142*, 1582–1592.

Kanatsu-Shinohara, M., Ogonuki, N., Inoue, K., Miki, H., Ogura, A., Toyokuni, S., and Shinohara, T. (2003). Long-term proliferation in culture and germline transmission of mouse male germline stem cells. Biol. Reprod. *69*, 612–616.

Kuroki, S., Akiyoshi, M., Ideguchi, K., Kitano, S., Miyachi, H., Hirose, M., Mise, N., Abe, K., Ogura, A., and Tachibana, M. (2015). Development of a general-purpose method for cell purification using Cre/loxP-mediated recombination. Genesis *53*, 387–393.

Marui, A., Tabata, Y., Kojima, S., Yamamoto, M., Tambara, K., Nishina, T., Saji, Y., Inui, K., Hashida, T., Yokoyama, S., et al. (2007). A novel approach to therapeutic angiogenesis for patients with

critical limb ischemia by sustained release of basic fibroblast growth factor using biodegradable gelatin hydrogel: an initial report of the phase I-IIa study. Circ. J. *71*, 1181–1186.

Meng, X., Lindahl, M., Hyvönen, M.E., Parvinen, M., de Rooij, D.G., Hess, M.W., Raatikainen-Ahokas, A., Sainio, K., Rauvala, H., Lakso, M., et al. (2000). Regulation of cell fate decision of undifferentiated spermatogonia by GDNF. Science *287*, 1489–1493.

Mullaney, B.P., and Skinner, M.K. (1992). Basic fibroblast growth factor (bFGF) gene expression and protein production during pubertal development of the seminiferous tubule: follicle-stimulating hormone-induced Sertoli cell bFGF expression. Endocrinology *131*, 2928–2934.

Nagai, R., Shinomura, M., Kishi, K., Aiyama, Y., Harikae, K., Sato, T., Kanai-Azuma, M., Kurohmaru, M., Tsunekawa, N., and Kanai, Y. (2012). Dynamics of GFRα1-positive spermatogonia at the early stages of colonization in the recipient testes of W/Wv male mice. Dev. Dyn. *241*, 1374–1384.

Nagano, M., Avarbock, M.R., and Brinster, R.L. (1999). Pattern and kinetics of mouse donor spermatogonial stem cell colonization in recipient testes. Biol. Reprod. *60*, 1429–1436.

Nakagawa, T., Sharma, M., Nabeshima, Y., Braun, R.E., and Yoshida, S. (2010). Functional hierarchy and reversibility within the murine spermatogenic stem cell compartment. Science *328*, 62–67.

Sariola, H., and Saarma, M. (2003). Novel functions and signalling pathways for GDNF. J. Cell Sci. *116*, 3855–3862.

Smith, E.P., Hall, S.H., Monaco, L., French, F.S., Wilson, E.M., and Conti, M. (1989). A rat Sertoli cell factor similar to basic fibroblast growth factor increases c-fos messenger ribonucleic acid in cultured Sertoli cells. Mol. Endocrinol. *3*, 954–961.

Sugimoto, R., Nabeshima, Y., and Yoshida, S. (2012). Retinoic acid metabolism links the periodical differentiation of germ cells with the cycle of Sertoli cells in mouse seminiferous epithelium. Mech. Dev. *128*, 610–624.

Suzuki, H., Sada, A., Yoshida, S., and Saga, Y. (2009). The heterogeneity of spermatogonia is revealed by their topology and expression of marker proteins including the germ cell-specific proteins Nanos2 and Nanos3. Dev. Biol. *336*, 222–231.

Tabata, Y., Hijikata, S., Muniruzzaman, M., and Ikada, Y. (1999). Neovascularization effect of biodegradable gelatin microspheres incorporating basic fibroblast growth factor. J. Biomater. Sci. Polym. Ed. *10*, 79–94.

Tadokoro, Y., Yomogida, K., Ohta, H., Tohda, A., and Nishimune, Y. (2002). Homeostatic regulation of germinal stem cell proliferation by the GDNF/FSH pathway. Mech. Dev. *113*, 29–39.

Takashima, S., Kanatsu-Shinohara, M., Tanaka, T., Morimoto, H., Inoue, K., Ogonuki, N., Jijiwa, M., Takahashi, M., Ogura, A., and Shinohara, T. (2015). Functional differences between GDNF-dependent and FGF2-dependent mouse spermatogonial stem cell self-renewal. Stem Cell Reports *4*, 489–502.

Uchida, A., Kishi, K., Aiyama, Y., Miura, K., Takase, H.M., Suzuki, H., Kanai-Azuma, M., Iwamori, T., Kurohmaru, M., Tsunekawa, N., et al. (2016). In vivo dynamics of GFRα1-positive spermatogonia stimulated by GDNF signals using a bead transplantation assay. Biochem. Biophys. Res. Commun. *476*, 546–552.

Ueda, H., Hong, L., Yamamoto, M., Shigeno, K., Inoue, M., Toba, T., Yoshitani, M., Nakamura, T., Tabata, Y., and Shimizu, Y. (2002). Use of collagen sponge incorporating transforming growth factor-beta1 to promote bone repair in skull defects in rabbits. Biomaterials *23*, 1003–1010.

Uehara, M., Yashiro, K., Mamiya, S., Nishino, J., Chambon, P., Dolle, P., and Sakai, Y. (2007). CYP26A1 and CYP26C1 cooperatively regulate anterior-posterior patterning of the developing brain and the production of migratory cranial neural crest cells in the mouse. Dev. Biol. *302*, 399–411.

Yamamoto, M., Ikada, Y., and Tabata, Y. (2001). Controlled release of growth factors based on biodegradation of gelatin hydrogel. J. Biomater. Sci. Polym. Ed. *12*, 77–88.

Yamamoto, M., Takahashi, Y., and Tabata, Y. (2006). Enhanced bone regeneration at a segmental bone defect by controlled release of bone morphogenetic protein-2 from a biodegradable hydrogel. Tissue Eng. *12*, 1305–1311.

Zhang, Y., Wang, S., Wang, X., Liao, S., Wu, Y., and Han, C. (2012). Endogenously produced FGF2 is essential for the survival and proliferation of cultured mouse spermatogonial stem cells. Cell Res. *22*, 773–776.

Zhou, M., Sutliff, R.L., Paul, R.J., Lorenz, J.N., Hoying, J.B., Haudenschild, C.C., Yin, M., Coffin, J.D., Kong, L., Kranias, E.G., et al. (1998). Fibroblast growth factor 2 control of vascular tone. Nat. Med. *4*, 201–207.

Zohni, K., Zhang, X., Tan, S.L., Chan, P., and Nagano, M.C. (2012). The efficiency of male fertility restoration is dependent on the recovery kinetics of spermatogonial stem cells after cytotoxic treatment with busulfan in mice. Hum. Reprod. *27*, 44–53.

Stem Cell Reports, Volume *10*

Supplemental Information

FGF2 Has Distinct Molecular Functions from GDNF in the Mouse Germline Niche

Kaito Masaki, Mizuki Sakai, Shunsuke Kuroki, Jun-Ichiro Jo, Kazuo Hoshina, Yuki Fujimori, Kenji Oka, Toshiyasu Amano, Takahiro Yamanaka, Makoto Tachibana, Yasuhiko Tabata, Tanri Shiozawa, Osamu Ishizuka, Shinichi Hochi, and Seiji Takashima

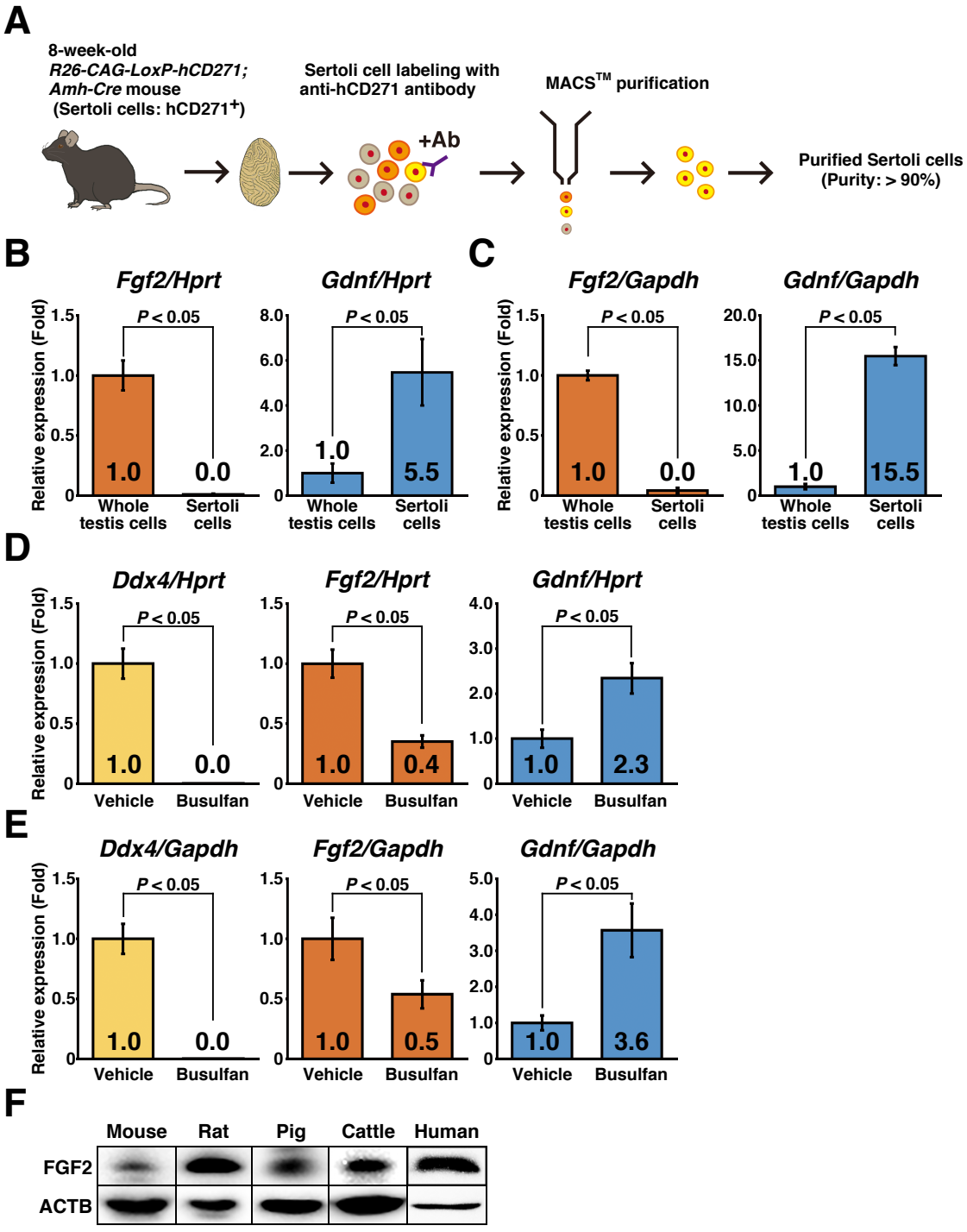

Figure S1, related to Figures 1 and 4. FGF2 expression in the testis. (A) Flow chart of Sertoli cell purification from an 8-week-old mouse testis. (B and C) qRT-PCR analysis of *Fgf2* expression in Sertoli cells. Whole testis cells before MACS™ purification and purified testis cells were compared. After normalization to *Hprt* (B) or *Gapdh* (C) expression, values of whole testis cells were set to 1.0 (n = 3 experiments using individual mice). Results were presented as means of values ± standard error of the mean. (D and E) qRT-PCR analysis of *Fgf2* expression in germ cell-depleted testes. Busulfan- and vehicle-treated testes were compared. After

normalization to *Hprt* (D) or *Gapdh* (E) expression, values of vehicle-treated testes were set to 1.0 (Vehicle, n = 5 testes from individual mice; Busulfan, n = 6 testes from individual mice). Results were presented as means of values ± standard error of the mean. (F) Western blot analysis of FGF2 in testes of mammals including mice, rats, pigs, cattle, and humans. ACTB was analyzed as a loading control. Typical blots from multiple experiments using independent samples are shown. $P < 0.05$ was considered as statistically significant (Student's *t*-test, B to E).

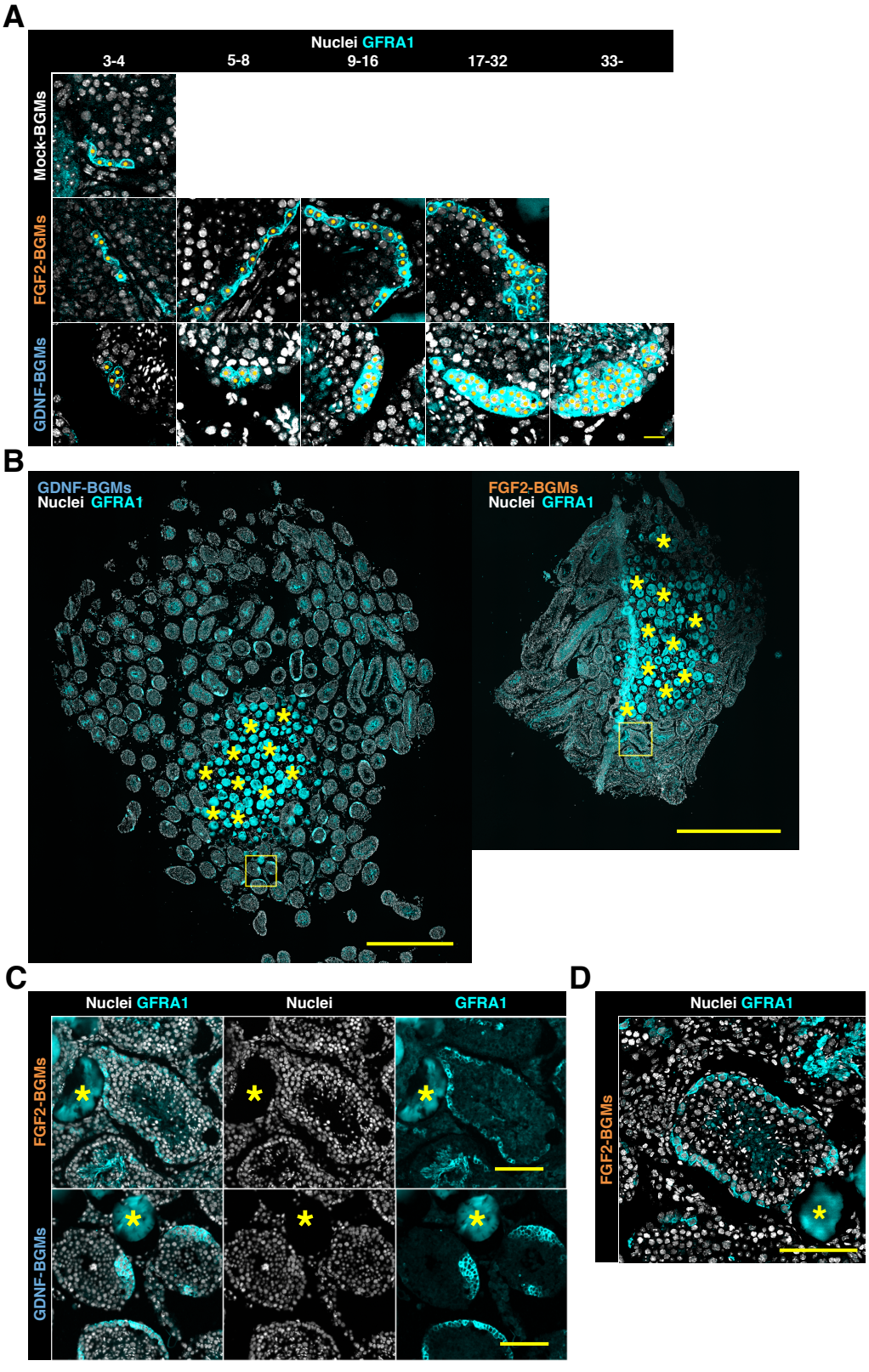
A
Nuclei GFRA1
3-4
5-8
9-16
17-32
33-
Mock-BGMs
FGF2-BGMs
GDNF-BGMs
B
GDNF-BGMs
Nuclei GFRA1
FGF2-BGMs
Nuclei GFRA1
C
Nuclei GFRA1
Nuclei
GFRA1
FGF2-BGMs
GDNF-BGMs
D
Nuclei GFRA1
FGF2-BGMs

Figure S2, related to Figure 1. GFRA1 expression in biodegradable gelatin microsphere (BGM)-treated mouse testes. Immunofluorescence image of BGM-transplanted testes at 10 days after transplantation. GFRA1 signals and nuclei are visualized by cyan and grey, respectively. (A) Typical images of large $GFRA1^+$ clusters classified by the number of $GFRA1^+$ spermatogonia. Yellow points indicate the spermatogonia forming cluster. (B) Overview of the testis at 10 days after transplantation of GDNF-BGMs (left) or FGF2-BGMs (right). Large $GFRA1^+$ clusters were often found around transplanted BGMs (marked with yellow asterisks). High power magnification images of regions indicated by yellow squares are shown in (C). (C) High power magnification views of large spermatogonial clusters observed in (B). Asterisks mark transplanted BGMs. (D) Most extreme case of FGF2-BGM treatment. The entire circumference of the seminiferous tubule was surrounded by $GFRA1^+$ spermatogonia. Asterisk indicates a transplanted FGF2-BGM. Bars = 20 μm (A), 1 mm (B), and 100 μm (C and D).

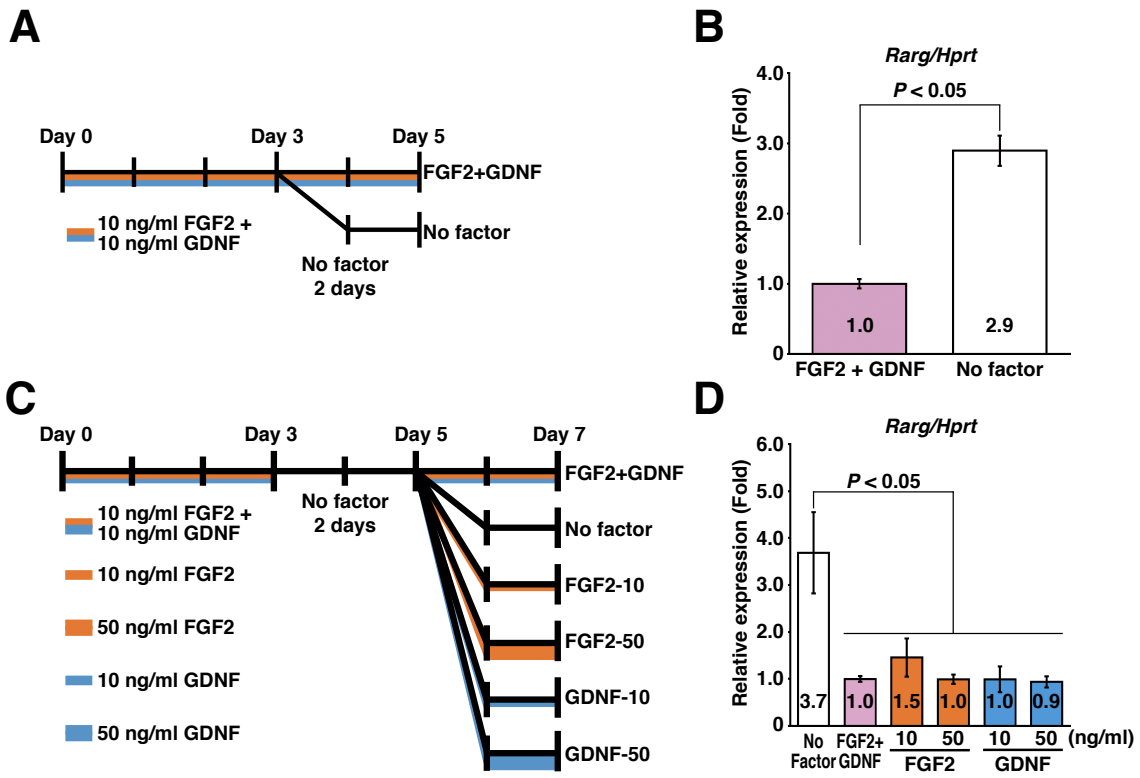

Figure S3, related to Figure 2. Both FGF2 and GDNF suppress *Rarg* expression in germline stem (GS) cells. GS cells were cultured on laminin-coated dishes under the conditions shown in (A) and (C), and then analyzed for *Rarg* expression by qRT-PCR. (A) GS cell culture conditions to assess the effects of FGF2 and GDNF. (B) qRT-PCR results of experiments shown in (A). After normalization to *Hprt* expression, the value of FGF2 + GDNF was set to 1.0 (n = 8 independent cultures for each group). Results were presented as means of values ± standard error of the mean. $P < 0.05$ was considered as statistically significant (Student's *t*-test). (C) GS cell culture conditions to assess the concentrations of FGF2 and GDNF. (D) qRT-PCR results of experiments shown in (C). After normalization to *Hprt* expression, the value of FGF2 + GDNF was set to 1.0 (n = 6 independent cultures for each group). Results were presented as means of values ± standard error of the mean. $P < 0.05$ was considered as statistically significant (one-way analysis of variance followed by Tukey's honest significant difference test).

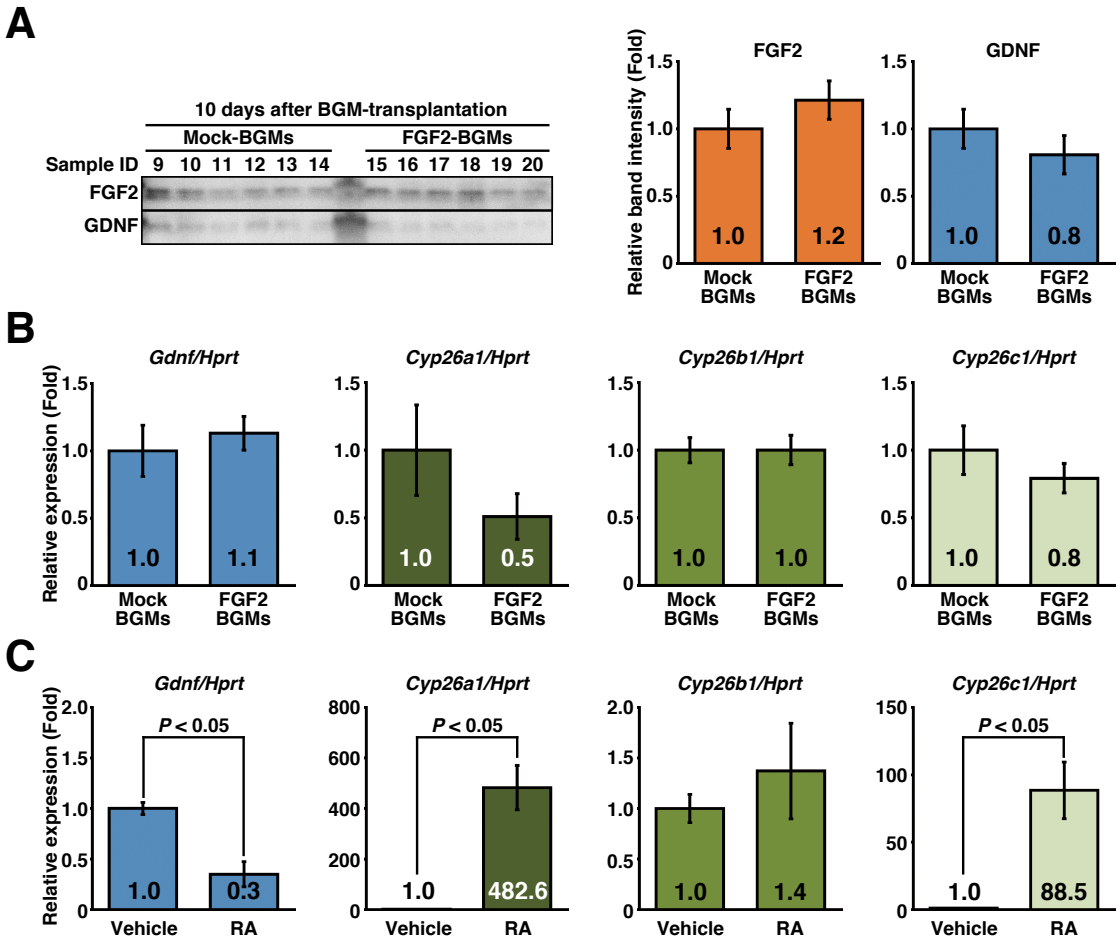

Figure S4, related to Figure 3. Functions of FGF2 and RA in the germline niche. (A) Western blot analyses of testes at 10 days after BGM treatment. Band intensities of Mock-BGM-treated testes were set to 1.0. (n = 6 testes for each condition). There was no significant difference in FGF2 levels between Mock-BGM- and FGF2-BGM-treated testes. Results were presented as means of values ± standard error of the mean. (B) qRT-PCR analysis of samples subjected to western blotting in (A). After normalization to *Hprt* expression, values of the Mock-BGM group were set to 1.0 (n = 6 testes for each condition). Results were presented as means of values ± standard error of the mean. (C) RA functions in the germline niche. At 4 weeks after busulfan treatment (44 mg/kg body weight), 7-week-old mice were further treated with RA (750 μg per mouse by intraperitoneal injection) or the vehicle. Testes were harvested at 11 hours after treatment and then subjected to qRT-PCR analysis. After normalization to *Hprt* expression, values of the vehicle group were set to 1.0 (n = 4 testes from individual mice for each condition). Results were presented as means of values ± standard error of the mean. $P < 0.05$ was considered as statistically significant (Student's *t*-test).

Table S1, related to Figures 1, 3, S1, S2, and S4. Antibodies used in this study

Antibody	Company
Primary antibody	
Goat anti-rat GFRA1 antibody (AF560)	R&D Systems, Inc., Minneapolis, MN
Rabbit anti-BrdU antibody (NBP2-14890)	Novus Biologicals, Littleton, CO
Rabbit anti-PLZF antibody (sc-22839)	Santa Cruz Biotechnology, Dallas, TX
Rabbit anti- RARG monoclonal antibody (#8965)	Cell Signaling Technology, Danvers, MA
Rabbit anti-mouse GDNF antibody (sc-328)	Santa Cruz Biotechnology
Rabbit anti-mouse FGF2 antibody (sc-79)	Santa Cruz Biotechnology
Rat anti-human CD271 monoclonal antibody (Clone ME20.4-1.H4, 130-091-883)	Miltenyi Biotec GmbH, Bergisch Gladbach, Germany
Mouse anti-ACTB monoclonal antibody (Clone 2F3, 013-24553)	Wako Pure Chemical Indutries, Osaka, Japan
Secondary antibody	
Alexa Fluor 488-conjugated donkey anti-rabbit IgG (A-21206)	Thermo Fischer Scientific, Waltham, MA
Alexa Fluor 555-conjugated donkey anti-rabbit IgG (A-21432)	Thermo Fischer Scientific
Alexa Fluor 647-conjugated donkey anti-goat IgG (A-21447)	Thermo Fischer Scientific
Horseradish peroxidase-conjugated goat anti-mouse IgG (#7076)	Cell Signaling Technology
Horseradish peroxidase-conjugated goat anti-rabbit IgG (#7074)	Cell Signaling Technology

Table S2, related to Figures 2, 3, S1, S3, and S4. Primers for qRT-PCR

Gene	Forward primer	Reverse primer
Cyp26a1	TGACCCGCAATCTCTTCTCT	GAGGAGCTCTGTTGACGATTG
Cyp26b1	TGGTCACTGGTTGCTACAGG	TGGGCAGGTAGCTCTCAAGT
Cyp26c1	CAAAATCCAGCAGGAGCTGT	AACCGTCCAGTTCAAAGGTG
Ddx4	CAGGCAATGGTGACACTTACC	ATGGAGTCCTCATCCTCTGG
Fgf2	CCAACCGGTACCTTGCTATG	TATGGCCTTCTGTCCAGGTC
Gapdh	AACTTTGGCATTGTGGAAGG	CACATTGGGGGTAGGAACAC
Gdnf	GCCACTTGGAGTTAATGTCC	CTTCGAGAAGCCTCTTACCG
Hprt	GCTGGTGAAAAGGACCTCT	CACAGGACTAGAACACCTGC
Rarg	AGGTCACCAGAAATCGATGC	CTGGCAGAGTGAGGGAAAAG

Supplemental experimental procedures

Animals, treatments, and testis tissues

Male C57BL/6NCrSlc (B6) mice were purchased from Japan SLC (Shizuoka, Japan). Seven-week-old mice were used as recipients of BGM transplantation. After the operation, recipients were administered with BrdU via water (0.5 mg/ml) *ad libitum* until sacrifice. Three-week-old mice were treated with a single intraperitoneal injection of 44 mg/kg body weight busulfan (Sigma-Aldrich, St Louis, MO) to deplete germ cells and then used as recipients of BGM transplantation and RA treatment as described below. For gene expression analysis of germ cell-depleted mice, 4-week-old mice were treated with busulfan (44 mg/kg body weight) and then subjected to qRT-PCR analysis at 8 weeks of age. For RA treatment, all-trans RA (Sigma-Aldrich) was dissolved in a 10% dimethylsulfoxide-sesame oil (Nacalai Tesque, Inc., Kyoto, Japan) solution and then injected intraperitoneally into busulfan-treated 7-week-old mice at 750 μg per mouse. Testes were harvested at 11 hours after treatment. 8-week-old male BN/SsNSlc rats were olso purchased from Japan SLC. Pig and cattle testes were collected at the time of castration to improve meat quality and growth rates at The Nagano Prefectural Livestock Experimental Station. Castrations were conducted at 5 months (cattle) and 8 weeks (pigs) of age. The institutional animal care and use committee of Shinshu University approved all animal experimentation protocols (Approval No. 260013 and No. 280120). Human testis tissues without pathological lesions were obtained and subjected to the experiments in accordance with the institutional ethics review board of Shinshu University to use human-derived material (Test No. 3039), and the institutional ethics review board of Nagano Red Cross Hospital to use human-derived material (Nagano-Byo-Ki Approval No. 25). Written consent was obtained following the committee-approved protocol before tissue collection.

Transplantation of biodegradable gelatin microspheres (BGMs)

Growth factor-adsorbed BGMs were transplanted into the testicular interstitium of recipient mice using a syringe with a 25 G needle (Terumo corporation, Tokyo, Japan). Male C57BL6/NCrSlc mice at 7 weeks of age (Japan SLC, Hamamatsu, Japan) with or without 44 mg/kg body weight busulfan (Sigma, St. Louis, MA) treatment at 3 weeks of age were used as recipients for BGM injection. For experiments shown in Figure 1, mice were administrated BrdU via water (0.5 mg/ml, Sigma) *ad libitum* until sacrifice. At 1 or 10 days after the procedure, mice were sacrificed and testes were harvested for analyses.

Enrichment of Sertoli cells

Sertoli cells were enriched from *R26-CAG-LoxP-hCD271; Amh-Cre* mice with a B6 background at Tokushima University under approval of the institutional animal care and use committee of Tokushima University (experimental number 14,108) (Kuroki et al., 2015). In brief, after removing the tunica albuginea, testis tissue from 8-week-old adult mice was digested with collagenase followed by trypsin-EDTA (Sigma) digestion. Resultant testis cells were further treated with collagenase, hyaluronidase, and a trypsin inhibitor. Single cell suspensions were subjected to MACS (Miltenyi Biotec GmbH, Bergisch Gladbach, Germany) using an anti-human CD271 antibody (Miltenyi Biotec GmbH) (See also Table S1).

qRT-PCR

Total RNA was prepared using Sepasol-RNA I Super G (Nacalai Tesque, Inc.). To synthesize first-strand cDNA, RNA samples were subjected to RT reactions using ReverTra Ace with gDNA remover (TOYOBO, Osaka, Japan). Resultant cDNA samples were analyzed by qRT-PCR using SYBR Premix Ex Taq II with Thermal Cycler Dice® Real Time System TP800 (TAKARA BIO Inc., Shiga, Japan). The qRT-PCR conditions were 95°C for 1 minutes followed by 40 cycles of 95°C for 15 seconds, 55°C for 30 seconds, and 72°C for 30 seconds, followed by a melting curve program. Each qRT-PCR was run in duplicate. Ct values were calculated by second derivative maximum method on Thermal Cycler Dice® Real Time System Software Version 5.10 (TAKARA BIO Inc.). The standard curve method was applied to determine the absolute quantity. Standard cDNA stock for absolute quantitation was prepared from PCR product using FastGeneTM Gel/PCR Extraction Kit (Nippon Genetics Co. Ltd., Tokyo, Japan). For data evaluation, after normalization to *Hprt* or *Gapdh* expression, values of the control group were set to 1.0. Primers used in this study are listed in Table S2.

Immunofluorescence staining

Harvested testes were fixed with 4% paraformaldehyde in PBS (-) for 4 hours at 4°C. After overnight incubation in 30% sucrose/PBS (-) at 4°C, tissues were embedded in Tissue-Tek OCT compound (Sakura Finetek, Tokyo, Japan) and processed for cryosectioning at 8 μm thickness. After permeabilization with 0.1% Triton-X 100 (Sigma) in ice-cold PBS (-) for 10 minutes followed by blocking with 10% donkey serum (Jackson ImmunoResearch Laboratories, Inc., West Grove, PA), sections were incubated with a primary antibody overnight at 4°C. Sections were further incubated with a secondary antibody at room temperature for 1 hour. Hoechst 33342 (Sigma) was used for nuclear counterstaining. Images were captured by confocal laser scanning microscopy (FV1000-D; Olympus, Tokyo, Japan) or All-in-one fluorescence microscopy (BZ-X700, KEYENCE, Osaka, Japan). Collected images were manually (FV-1000D) or automatically (BZ-X700) joined to reconstruct an entire image of testicular cross sections. Only cross sections containing transplanted BGMs were analyzed. Antibodies used in this study are listed in Table S1.

Cell culture

GS cells, F-SPG, and G-SPG were originally established at T. Shinohara's laboratory and kindly provided. Culture medium used in this study was based on reports by Kanatsu-Shinohara et al (2003) for GS cells and Takashima et al. (2015) for F-SPG and G-SPG. GS cells were maintained by treatment with 10 ng/ml rat GDNF (Peprotech, London, UK) and 10 ng/ml human FGF2 (Peprotech). G-SPG were cultured with 10 ng/ml rat GDNF only, whereas F-SPG were cultured with 10 ng/ml human FGF2 only. All cell lines were maintained on laminin-coated dishes for more than 2 weeks and then subjected to qRT-PCR analysis. The concentrations of growth factors in experiments are indicated in the figures (Figures 2A, S3A, and S3C).

Western blotting

Collected testis samples were stored at -80°C and then lysed in lysis buffer consisting of 25 mM Tris-HCl (pH 8.0), 0.2% Triton X-100, 2.5 mM EDTA, 1 mM dithiothreitol (Sigma), and a protease inhibitor cocktail (Nacalai Tesque, Inc.). Protein concentrations were determined by BCA™ Protein Assay Kit-Reducing Agent Compatible (Thermo Fischer Scientific, Waltham, MA). After denaturation by mixing with sample buffer containing sodium dodecyl sulfate (SDS) and 2-mercaptoethanol followed by boiling, samples (60 μg protein/lane) were separated by SDS-polyacrylamide gel electrophoresis (SDS-PAGE). In case of FGF2 detection in human testes, samples were loaded at 100 μg protein/lane. Separated proteins were transferred onto polyvinylidene fluoride membranes (Amersham Hybond P 0.45: GE Healthcare, Buckinghamshire, UK), and then incubated with primary antibodies. After incubation with a horseradish peroxidase-conjugated secondary antibody, immunoreactive bands were detected using Lumi GLO reagent (Cell Signaling Technology, Inc., Danvers, MA) and a *LuminoGraph* I luminescence imager (ATTO CORPORATION, Tokyo, Japan). The signal intensities of specific bands were quantitatively analyzed by ImageJ (http://imagej.nih.gov/ij/index.html). Values of Mock-BGM samples were set to 1.0. The antibodies used are listed in Table S1.